Published in final edited form as:

Mol Cell Endocrinol. 2017 September 05; 452: 1–14. doi:10.1016/j.mce.2017.04.005.

Exposure of decidualized HIESC to low oxygen tension and leucine deprivation results in increased IGFBP-1 phosphorylation and reduced IGF-I bioactivity

Majida Abu Shehab[a], **Kyle Biggar**[b,1], **Sahil Sagar Singal**[b], **Karen Nygard**[c], **Shawn Shun-Cheng Li**[b], **Thomas Jansson**[d], and **Madhulika B. Gupta**[a,b,e,*]

[a]Children's Health Research Institute, University of Western Ontario, London, Ontario, Canada

[b]Department of Biochemistry, University of Western Ontario, London, Ontario, Canada

[c]Department of Biotron, University of Western Ontario, London, Ontario, Canada

[d]Department of Obstetrics & Gynecology, University of Colorado Anschutz Medical Campus, Aurora, CO, USA

[e]Department of Pediatrics, University of Western Ontario, London, Ontario, Canada

Abstract

Phosphorylation of decidual IGFBP-1 enhances binding of IGF-I, limiting the bioavailability of this growth factor which may contribute to reduced placental and fetal growth. The mechanisms regulating decidual IGFBP-1 phosphorylation are incompletely understood. Using decidualized human immortalized endometrial stromal cells we tested the hypothesis that low oxygen tension or reduced leucine availability, believed to be common in placental insufficiency, increase the phosphorylation of decidual IGFBP-1. Multiple reaction monitoring-MS (MRM-MS) was used to quantify IGFBP-1 phosphorylation. MRM-MS validated the novel phosphorylation of IGFBP-1 at Ser58, however this site was unaffected by low oxygen tension/leucine deprivation. In contrast, significantly elevated phosphorylation was detected for pSer119, pSer98/pSer101 and pSer169/pSer174 sites. Immunoblotting and dual-immunofluorescence using phosphosite-specific IGFBP-1 antibodies further demonstrated increased IGFBP-1 phosphorylation in HIESC under both treatments which concomitantly reduced IGF-I bioactivity. These data support the hypothesis that down regulation of IGF-I signaling links decidual IGFBP-1 hyperphosphorylation to restricted fetal growth in placental insufficiency.

Keywords

Hyperphosphorylation; Cellular stress-stimuli; IGF bioavailability; FGR; MRM-MS; Dual immunofluorescence; immunocytochemistry

[*]Corresponding author. Departments of Pediatrics and Biochemistry, Children's Health Research Institute, University of Western Ontario, VRL Room A5-136 (WC), 800 Commissioners Road E., London, ON N6C 2V5, Canada. mbgupta@uwo.ca (M.B. Gupta).

[1]Institute of Biochemistry, Carleton University, Ottawa, ON, Canada.

Disclosure statement

Authors have nothing to declare.

1. Introduction

Fetal growth restriction (FGR) increases the risk of perinatal complications and is linked to the development of obesity, diabetes and cardiovascular disease later in life (Gluckman et al., 2008). However, the pathophysiology underlying FGR is not yet clearly understood. The insulin-like growth factor (IGF) system is a critical regulator of fetal growth (Baker et al., 1993). Short term maternal undernutrition in animal models leads to cessation of fetal growth associated with reduced fetal IGF-I levels and altered circulating concentrations of IGF binding proteins (IGFBPs) (Gluckman and Pinal, 2003; Baxter, 2000). The activity of IGFs is strongly modulated by IGFBPs. Because binding of IGFs to IGFBPs prevents association of the growth factor to its receptors, IGFBPs can inhibit the stimulatory actions of IGFs on cellular proliferation, migration and differentiation (Baxter, 2000). Conversely, binding of IGFBPs to IGFs can in some situations have stimulatory effects, possibly by bringing the growth factor in close proximity to the receptor, therefore augmenting the interaction (Baxter, 2000).

Overexpression of hepatic IGFBP-1 in transgenic mice has been shown to cause a 15–20% reduction in birth weight (Watson et al., 2006), providing strong evidence that hepatic IGFBP-1 is an important endocrine regulator of fetal growth. Low oxygen tension (hypoxia) strongly induces IGFBP-1 protein and mRNA expression levels which plays an important role in regulating embryonic/fetal growth (Kajimura et al., 2005). A role for hypoxia-inducible factor 1 (HIF-1) and hypoxia-response element 1 (HRE1) in induction of IGFBP-1 gene expression has been proposed previously to restrict IGF-mediated fetal growth (Tazuke et al., 1998). IGFBP-1 is elevated in fetuses with long-term, chronic hypoxia. Low oxygen tension triggers IGFBP-1 secretion also in hepatocellular carcinoma HepG2 cells (Tazuke et al., 1998) as well as in primary hepatocytes isolated from human fetuses (Popovici et al., 2001). In addition, reduced amino acid availability also increases the expression of IGFBP-1 (Averous et al., 2005). These findings implicate stress-responsive alterations in fetal IGFBP-1/IGF-I system to play an important role in the development of FGR.

Central to IGF-I bioactivity in FGR is the phosphorylation status (sites and degree) of IGFBP-1. Given that the affinity of phosphorylated IGFBP-1 for IGF-I is greater than that of non-phosphorylated IGFBP-1, phosphorylated IGFBP-1 typically inhibits the IGF-I/IGF-1R interaction (Jones et al., 1993a). We have previously demonstrated that IGFBP-1 phosphorylation in HepG2 cells is induced in response to both leucine deprivation and hypoxia and increases its affinity for IGF-I up to 300-fold (Seferovic et al., 2009). This increase in IGF-I affinity results in a pronounced inhibition of cellular proliferation and inhibition of IGF-I bioactivity during periods of cellular stress (Seferovic et al., 2009; Damerill et al., 2016); these data are consistent with several literature reports showing that phosphorylation of IGFBP-1 more potently inhibits IGF-I stimulated cell proliferation, DNA synthesis, amino acid transport and apoptosis (Firth and Baxter, 2002). We have also previously reported that IGFBP-1 phosphorylation is markedly increased at three specific serine residues (Ser101, Ser119 and Ser169) in the amniotic fluid of human growth restricted fetuses (Abu Shehab et al., 2010). We also have shown that IGFBP-1 phosphorylation is increased in the fetal liver of FGR baboons (Abu Shehab et al., 2014).

Together these data indicate that changes in the phosphorylation status of fetal IGFBP-1 may directly contribute to abnormal fetal growth.

During implantation and early pregnancy ovarian hormones promote the morphological and functional transformation of endometrial stromal cells into decidua, which play an important role in regulating trophoblast invasion. The decidua is also the major source of maternal circulating IGFBP-1 (Martina et al., 1997; Gibson et al., 2001) and the decidua therefore controls the bioavailability of maternal IGF-I. Because maternal IGF-I is an important regulator of placental growth and function, including placental nutrient transport (Chellakooty et al., 2004), the decidua plays a critical role in modulating maternal-fetal resource allocation (Martina et al., 1997). A lack of normal increase in utero-placental blood flow results in placental insufficiency, which is a common cause of FGR. Placental insufficiency is believed to be associated with placental hypoxia and decreased levels of nutrients (Hutter et al., 2010). It is therefore possible that increased phosphorylation of decidual IGFBP-1 by hypoxia and nutrient deprivation may contribute to the restricted fetal growth indirectly by decreasing the bioavailability of IGF-I in the maternal circulation.

The gestational age related changes in phosphoisoform patterns in decidual explants have been reported previously (Martina et al., 1997), however, the status of IGFBP-1 phosphorylation at specific sites is currently unknown and there are no previous reports of mechanisms regulating decidual IGFBP-1 phosphorylation in normal pregnancy or in association to placental insufficiency. We tested the hypothesis that decreased oxygen or leucine availability, believed to be common in placental insufficiency, increase the phosphorylation of decidual IGFBP-1. We used decidualized human immortalized endometrial stromal cell (HIESC) (Chapdelaine et al., 2006) as a model system for determining the effects of hypoxia and leucine deprivation on decidual IGFBP-I phosphorylation. Multiple reaction monitoring mass spectrometry (MRM-MS) was applied as a targeted approach (Damerill et al., 2016) to quantify the site-specific IGFBP-1 phosphorylation in decidualized HIESC. Our extensively validated phosphosite-specific IGFBP-1 antibodies (Abu Shehab et al., 2014; Abu Shehab et al., 2013) were utilized for immunoblot analysis as well as subcellular localization using dual immunofluorescence immunocytochemistry (ICC). Moreover, inhibitory effects of IGFBP-1 hyperphosphorylation on IGF-I bioactivity were assessed using IGF-1R autophosphorylation (Abu Shehab et al., 2013). We further tested the impact of changes in IGFBP-1 phosphorylation on IGF-I signaling activity to establish the biological/physiological relevance of the overall findings in this study.

2. Materials and methods

2.1. Cell culture and in vitro decidualization

HIESC (a gift, Dr. M Fortier, U Laval, Canada) were plated in 12 well plates at 75% confluence and cultured in RPMI 1640 medium without phenol red (Life Technologies, Burlington, ON) enriched with 10% fetal bovine serum (FBS) and 50 IU penicillin-streptomycin (Life Technologies, Burlington, ON) at 37 °C with 5% CO_2. After 24 h, the cell monolayer was washed in phosphate-buffered saline (PBS). For decidualization, media was replaced with RPMI 1640 media but containing 2% dialyzed FBS (stripped using

Dextran Coated Charcoal (DCC; Sigma Aldrich, ST Louis MO), 0.5 mM 8-bromo cAMP (Cayman Chemicals, Ann Arbor, MI) and 1.0 μM medroxyprogesterone acetate (MPA) (Pfizer Canada, Kirkland, Quebec). The media was changed every 48 h. After six days of decidualization, the media was collected for the assessment of IGFBP-1 secretion and phosphorylation, whereas cells were lysed in lysis buffer (Cell Signaling Technologies, Danvers, MA) and studied as described below.

2.2. Changes in morphology following decidualization of HIESC by shape index calculation

The morphological characteristic of HIESC was determined before and after decidualization using the approach of calculating the shape index as described (Kajihara et al., 2014). Phase contrast images were captured 6 days after decidualization (treatment with cAMP + MPA). Individual cells (50 cells) were outlined from three cultures (n = 3) for control and treated cells and the roundness factor was determined using Image Pro Premier software. The shape index formula used was as reported by Kajihara et al. (2014) (4pi x area/perimeter^2). A circular object would have a shape index of 1 whereas a straight line has an index of 0.

2.3. Decidualized HIESC culture in low-oxygen tension

After six days of decidualization, HIESC were exposed to low-oxygen tension (1% O_2). The cells were cultured in decidualization media and then placed either in incubator air (normoxia) or a sealed hypoxia chamber, filled with a 1% O_2, 5% CO_2, balanced N_2 gas mixture (Praxair Canada Ltd) for 15 min to ensure saturation. Thereafter, the sealed chamber was placed in a tissue culture incubator at 37 °C on an orbital shaker for 24 h. Based on our previous studies (Seferovic et al., 2009, 2011; Damerill et al., 2016; Seferovic and Gupta, 2016) utilizing a Hudson 5590 Oxygen Monitor (Hudson, Ventronics Division) the saturation of the O_2 in the chamber has been shown to remain consistent for up to 72 h. After treatment, the cell media and cell lysate were collected and stored at −80 °C for further analysis.

2.4. Leucine deprivation of decidualized HIESC

Cells were cultured in 12 well plates in decidualization media for six days. Subsequently, prior to harvesting, the cells were washed in PBS and cultured in DMEM F12 lacking the essential amino acid leucine (Leu 0 μM) as previously (Seferovic et al., 2009; Malkani et al., 2016, 2015). In the control treatment the cells were washed and cultured in DMEM/F12 media containing the standard amino acid concentrations including leucine (450 μM). After 24 h the cell media and the lysates were collected and stored at −80 °C and were analyzed as described below.

2.5. Immunoprecipitation of decidual IGFBP-1

Enrichment of IGFBP-1 from cell media was performed by immunoprecipitation (IP) using anti human IGFBP-1 monoclonal antibody (mAb 6303). Equal volume (3 mL) of cell media from decidualized HIESC under control conditions (normoxia) and standard amino acid concentration (450 μM Leu), in low-oxygen tension (1% O_2) and amino acid deprivation (0 μM Leu) for 24 h were buffer exchanged, concentrated and immunoprecipitated (IP) as we reported in our previous studies (Damerill et al., 2016; Abu Shehab et al., 2009). Equal

aliquots of the IP samples were tested on western blot for the detection of total and phosphorylated IGFBP-1. For MRM-MS analysis the IP samples were washed and digested in-solution as described below for the quantification of site specific IGFBP-1 phosphorylation.

2.6. MRM-MS analyses of IGFBP-1 phosphopeptides

We performed in-solution digestions using the IP samples of IGFBP-1 from cell media isolated from decidualized HIESC cultured in low-oxygen tension or leucine deprivation as previously described (Damerill et al., 2016; Malkani et al., 2016). In brief, the IGFBP-1 sample was first digested using endoproteinase Asp-N incubated overnight at 37 °C (Roche Diagnostics, Laval, QC, Canada) and followed by a subsequent digestion using trypsin (Roche Diagnostics) overnight at 37 °C following the manufacturers instruction. IGFBP-1 digests were subsequently analyzed by LC-MS/MS with a triple quadruple mass spectrometer (4000 QTRAP AB Sciex, Concord, ON, Canada) using methods that we previously optimised for the detection of site-specific IGFBP-1 phosphorylation (Damerill et al., 2016; Malkani et al., 2016). A NanoAcquity UPLC system (Waters, Milford, MA, USA) equipped with a C18 analytical column (1.7 μm, 75 μm × 200 mm) was used to separate the peptides at a flow rate of 300 nl/min and operating pressure of 8000 psi. Digested IGFBP-1 peptides were electrosprayed into the mass spectrometer, which monitored 98 transitions per sample with a dwelling time of 50 msec/transition (Supplemental Table S1). Relative changes in IGFBP-1 phosphorylation were determined by the total peak height of combined transitions. An internal IGFBP-1 peptide (NH_2-ALPGEQQPLHALTR-COOH) was used to normalize all phospho-IGFBP-1 data. For peptides with two possible phosphorylation sites, specific transitions used to distinguish single site phosphorylation from each other (specifically, y14, b6 and b9 ions for pS169 and pS174; y12 and b15 ions for pS98 and pS101). All the samples used for MRM-MS were analyzed two times using three pooled biological triplicates of IGFBP-1 isolated (IP) from equal volume of cell (HIESC) media (3 mL each from three different cultures).

2.7. Western blot analysis

Western blot analysis was performed as described (Abu Shehab et al., 2014). In brief, conditioned media was collected and cell lysates were centrifuged at 13,000 rpm (15,871 g) for 30 min, supernatants were collected and stored at −80 °C until used. The HIESC conditioned medium (3.0 mL) were buffer exchanged and concentrated 10x using Amicon Ultracell 10 K MWCO centrifugal filter devices (ThermoFisher Scientific). Equal aliquots of enriched conditioned media (10 μL) or a total of 30 μg cell lysate protein sample was resolved by SDS-PAGE and then transferred onto nitrocellulose membrane (Bio-Rad Laboratories). The membranes were blocked with 5% milk in Tris-buffered saline (w/v) plus 0.1% Tween 20 (v/v) for 1 h at room temperature. Blots were then washed (TBS-Tween-20, 0.1%) followed by incubation at 4 °C overnight with respective primary antibodies. Subsequently, blots were washed and exposed to corresponding HRP-conjugated secondary antibody for 1 h at room temperature and bands were visualized using Clarity Western ECL substrate (BioRad). Images were captured on VersaDoc Imaging System (Bio-Rad) and Quantity One imaging software (BioRad). Blots were further stripped using 50 mM Glycine buffer (pH 2.8), washed, blocked and reprobed using β-actin antibody as a loading control.

A densitometry analysis of the blots was performed by using Image lab software (BioRad). For each protein target, the mean (triplicate) intensity of the control sample bands was assigned an arbitrary value of 100. Subsequently, all individual control and treated densitometric values were reported relative to this value.

Using immunobot analysis, decidualization of cells was confirmed by ERα expression using ERα antibody (Cell Signaling Technologies). The expression of total and phosphorylated IGFBP-1 in cell media was detected using mAb (6303) antibody (Medix Biochemica, Finland), and our custom made phosphosite-specific (pSer101, pSer119 and pSer169) antibodies (YenZyme, CA, USA) respectively, that we have validated previously (Abu Shehab et al., 2014; Abu Shehab et al., 2013). The functional effect of changes in IGFBP-1 phosphorylation on IGF-1R autophosphorylation was tested by phospho IGF-1Rβ (Tyr 1135) antibody (Cell Signaling Technologies) (Abu Shehab et al., 2013). The effects of decidual IGFBP-1 phosphorylation on IGF-1R downstream signaling was determined by phospho IRS-I (Tyr 612) antibody (Invitrogen) and phospho Akt (Thr 308) antibody (Cell Signaling Technologies).

2.8. Dual immunofluorescence staining

HIESC were grown on Poly L Lysine (Cultrex) coated glass coverslips and were decidualized as described above. Cells were then cultured in low-oxygen tension and/or leucine deprivation for 24 h as described in detail previously and used for immunofluorescence analysis. After fixation with 1 mL of 4% paraformaldehyde for 1 h at 4 °C, the cells were washed with PBS (3 × 5 min) and then incubated for 10 min with 0.5% Triton X-100 to make them permeable. Following another set of three 5 min washes with PBS, the cells were blocked with Sniper using Dako Background Sniper (Biocare Medical, Concord, CA) for 10 min. Subsequently, ICC was performed and the cells were stained with primary antibodies (100 μL); three phosphorylated IGFBP-1 isoforms using custom made validated phosphosite-specific (pSer101, pSer119 and pSer169) antibodies (Abu Shehab et al., 2014; Abu Shehab et al., 2013) and mouse monoclonal Vimentin (Biocare Medical, Concord, CA) antibody. The phosphosite-specific IGFBP-1 antibodies were diluted to 1:1000 whereas vimentin mAb was diluted to 1:25 in Dako antibody diluent (Biocare Medical, Concord, CA). The primary antibodies were incubated at 4 °C for 24 h. All incubations were carried out in a humidified chamber. Cells were washed with PBS for 3 cycles of 5 min each. The cells were then conjugated with corresponding combinational secondary antibodies (100 μL), Alexa 568 (anti-rabbit) and Alexa 660 (anti-mouse) diluted to 1:400. Secondary antibody incubation was performed for 1 h at room temperature followed by three 5-min PBS washes. The cells were counter stained with DAPI (100 μL) (Life Technologies, Burlington ON) at 1:200 dil for 2 min. Cover slips were then mounted on to slides with 50 μL of Prolong Gold Diamond Mounting Media (Life Technologies, Burlington ON). Imaging was performed using an AxioImager Z1 Epifluorescent Microscope (Carl Zeiss Canada Ltd).

2.9. IGF-1 receptor autophosphorylation

The inhibitory effects of IGFBP-1 hyperphosphorylation on IGF-I bioactivity were assessed using IGF-1R autophosphorylation using IGF-1R overexpressing P6 cells (Abu Shehab et

al., 2013). Briefly, decidualized cell media from HIESC in low-oxygen tension and/or leucine deprivation treatments were buffer exchanged against serum free high glucose DMEM with Sodium pyruvate cell media, concentrated 10x using Amicon Ultracell 10 K MWCO centrifugal filter devices (Thermofisher Scientific). As shown in the methodological flow diagram (Fig. 11A), briefly, equal concentration of total IGFBP-1 (100 ng/mL) in the media were then incubated with recombinant human (rh) IGF-I (100 ng/ml) for 2 h at room temp rotating on a shaker. The IGF-I:IGFBP-1 complexes formed in media were utilized to treat P6 cells for 10 min at room temperature. The treatment was stopped by aspirating the media and cell lysis was performed using lysis buffer. The cell lysates were collected and stored at −80 °C to further test for IGF-1R activity using western immunoblot analysis using anti phospho-IGF-1Rβ (Tyr 1135) antibody (Cell Signaling Technology) (1: 1000 dilution). The membrane was stripped and re-probed with antibody for total anti IGF-1Rβ (Santa Cruz Biotechnology) at 1:1000 dilution. The densitometry of the phosphorylated IGF-1Rβ band was normalized to the band intensity of total IGF-1Rβ and finally to β-actin.

2.10. IGF-1 receptor downstream signaling

Equal aliquots of cell lysates (30 μg total protein) from decidualized HIESC cultured in low-oxygen tension and/or leucine deprivation were tested on western blot analysis for changes in IGF-1R downstream signaling activity. We determined the patterns of the insulin receptor substrate 1 (IRS-1) and its phosphorylation (at Tyr 612) (Invitrogen), and Akt levels and Akt phosphorylation (at Thr 308) (Cell Signaling Technologies) using western blot analysis as described above. After imaging, the blots were stripped and reprobed using total Akt and total IRS-1 antibodies. The density of both phosphorylated and total protein bands were normalized to β-actin.

2.11. Statistical analysis

All assays were run in triplicates from 3 independent experiments each with 3 or more HIESC biological replicates except for MRM/MS where the experiment was performed twice in triplicate each time. Data are presented as mean ± SEM. Statistical significances of differences between groups were determined using Student t-test or, in the case of the IGF-1R autophosphorylation assay, ANOVA followed by multiple comparison test and $P < 0.05$ was considered significant.

3. Results

3.1. Changes in HIESC morphology following decidualization

A combined treatment of cAMP + MPA from 24 h to day 6 of culture induced decidualization in HIESC, as suggested by the change in cell morphology from elongated spindle shape cells to ovoid shaped cells with large cytoplasm characteristics organized in a pavement-like morphology. Fig. 1 (A and B; 10x, C and D, 20x). Non-decidualized confluent HIESC remained spindle-shaped fibroblast like cells throughout the culture period.

The morphological characteristics of the cells before and after cAMP + MPA treatments were also determined using shape index analysis. The non-decidualized confluent HIESC

remained spindle/straight shaped and treatment with cAMP + MPA increased shape index by +340% above the control (Fig. 1E). Collectively, these findings provide morphological evidence for decidualization of HIESC following cAMP + MPA treatment.

3.2. IGFBP-1 secretion and phosphorylation confirm decidualization of HIESC

HIESCs express estrogen receptor (ERα), however upon decidualization a gradual and significant reduction (−57%) of expression was observed (Chapdelaine et al., 2006) as shown in Fig. 2A and B. The decidualization resulted in significantly increased secretion of IGFBP-1, which reached peak levels at 6 days of culture (Fig. 2C). Moreover, IGFBP-1 phosphorylation at Ser101, Ser119 and Ser169 was clearly detectable following 6-day treatment with cAMP + MPA (Fig. 2D). These observations represent functional evidence for successful decidualization.

3.3. MRM-MS detection of enhanced dually phosphorylated IGFBP-1 peptides

Site-specific phosphorylation of IGFBP-1 in human decidua under normal conditions or in response to cellular stress has not been studied previously. To identify/quantify the relative changes in sites of phosphorylation of decidual IGFBP-1 in response to hypoxia or leucine deprivation, we first investigated the changes at three known serine sites (Ser101, Ser119 and Ser169) (Damerill et al., 2016; Malkani et al., 2016). The HIESC conditioned media samples were analyzed by MRM-MS using an internal IGFBP-1 peptide to normalize data as described previously (Damerill et al., 2016). The phosphorylation sites within single or double phosphopeptides identified in relation to their relative retention time are summarized in Table 1. MRM-MS showed a +327% increase above the control of IGFBP-1 phosphorylation at Ser119 under low oxygen tension treatment (Fig. 3A). Similarly, treatment of HIESCs with leucine deprivation led to enhanced IGFBP-1 phosphorylation at Ser119 (+45% compared to control, Fig. 3B). The ion chromatograph in Fig. 3C shows the transitions used to validate the phosphorylation data on Ser119.

Moreover, our analyses showed a +220% increased phosphorylation at Ser98 and +310% enhanced phosphorylation at Ser101 singly, while the intensity of a doubly phosphorylated peptide with Ser98 + Ser101 was +230% higher in low-oxygen tension than in the control samples (Fig. 4A). In response to leucine deprivation, IGFBP-1 phosphorylation at Ser98 and Ser101 singly increased +43% and +60%, respectively as compared to the control (set as 100%), however the combined Ser98/Ser101 phosphorylation was not changed (Fig. 4B). Fig. 4C, D and E show representative ion chromatographs of the transitions used to validate the phosphorylation data on each site in each treatment.

Furthermore, the extracted ion chromatograph showing the transitions used to validate the phosphorylation at Ser169 + Ser174 in a doubly phosphorylated peptide represents unique peptide fragment ions (peptide transitions) that are specific to the pSer169/Ser174 sites. Relative quantitation of intensities showed +180% and +70% increase in phosphorylation of the doubly phosphorylated peptide pSer169 + pSer174 (Fig. 5A) in low-oxygen tension and in response to leucine deprivation respectively where each treatment was analyzed relative to that control (Fig. 5B). Our data also demonstrate that low-oxygen tension did not affect IGFBP-1 phosphorylation on single sites (Ser169 or Ser174) (Fig. 5A). However, leucine

deprivation treatment led to +78% and +54% enhanced phosphorylation of the single sites Ser169 and Ser174 respectively (Fig. 5B). Fig. 5C, D and E show representative ion chromatographs of the transitions used to validate the phosphorylation data on each site in each treatment.

3.4. MRM-MS detection of a novel IGFBP-1 (Ser58) phosphorylation

Further analysis revealed a novel IGFBP-1 phosphorylation site Ser58 at the N-terminal region of the protein (Fig. 6). The newly identified Ser58 in HIESC cultured under normal conditions was validated by the ion chromatograph showing the transitions used to confirm the presence of IGFBP-1 phosphorylation. The early elution time of the Ser58 phosphopeptide is likely indicative of an acidic nature (more negatively charged) as compared to other IGFBP-1 phosphopeptides in the samples (Table 1).

We further investigated Ser58 phosphorylation status of IGFBP-1 in HIESC cultured in low oxygen tension and leucine deprivation. We found that pSer58 site is responsive to neither of the two stimuli. It is possible that pSer58 under normal conditions is involved in regulating the bioavailability of IGF-I during healthy pregnancy allowing optimum fetal growth. Because our results confirmed that Ser58 is not affected by low oxygen or leucine deprivation treatments, additional data is not shown. Considering the functionality of this residue is not yet available, further structure and functional studies are necessary to assess its role in regulating IGF-I bioavailability in decidua or other cell types. It is possible that phosphorylation at Ser58 may be unique to the decidua to regulate IGF-I function.

3.5. Immunoblot analysis validated enhanced decidual IGFBP-1 phosphorylation

To validate data generated via MRM-MS, we applied conventional immunoblotting using IGFBP-1 isolated by IP from equal aliquots of cell media from decidualized HIESC cultured in low-oxygen tension and/or leucine deprivation. The data showed that low-oxygen tension treatment significantly increased total IGFBP-1 expression +47% ($P < 0.0023$; Fig. 7A). Additionally, hypoxia also significantly enhanced IGFBP-1 phosphorylation on Ser101 + 50%; $P < 0.0018$ (B), Ser119 + 38%; $P < 0.0269$ (C) and Ser169 + 40%; $P < 0.0001$ (D).

Leucine deprivation likewise resulted in significant increase in both total and phosphorylated IGFBP-1. Fig. 8 showed that total IGFBP-1 was enhanced +86%; $P < 0.0005$. A significant increase in site-specific IGFBP-1 phosphorylation was observed at Ser101+ 81%; $P < 0.0076$, Ser119 + 82%; $P < 0.0128$ and Ser169 + 71%; $P < 0.0017$ (Fig. 8B, C and D respectively) in response to leucine deprivation.

3.6. Dual immunofluorescence confirms co-expression of phosphorylated IGFBP-1 isoforms with vimentin

Dual immunofluorescence confocal microscopy using our custom IGFBP-1 phosphosite-specific antibodies (Abu Shehab et al., 2014; Abu Shehab et al., 2013) together with an anti-vimentin antibody confirmed that a significant number of decidual cells co-express IGFBP-1 phosphorylated at Ser101, Ser119 and Ser169 (Figs. 9 and 10). Anti-vimentin antibody reacts with the 57 kDa intermediate filament protein present in cells of mesenchymal origin and the strong vimentin staining, which was predominantly cytosolic, confirmed

mesenchymal characteristics of HIESCs (Fig. 9). Phospho-IGFBP-1 staining for each of the three phosphoisoforms overlaid vimentin staining and appeared to be present throughout the cytoplasm of HIESC. As our merged channel image depicts an overlap of green and red channels, suggests that phosphorylated IGFBP-1 is predominantly localized in the cytosol. Low oxygen tension enhanced IGFBP-1 phosphorylation at Ser101, Ser119 and Ser169 (representative data shown for pSer101) (Fig. 9). HIESC cultured under leucine deprivation showed pronounced increase in IGFBP-1 phosphorylation compared with leucine at all three phosphorylation sites (Fig. 10). These data (Figs. 9 and 10) although qualitative, are consistent with western blot as well as MRM-MS analysis suggesting that low oxygen tension and leucine deprivation led to pronounced increase in IGFBP-1 phosphorylation at Ser101, Ser119 and Ser169 compared with respective controls.

3.7. IGF-1R autophosphorylation is reduced by increased decidual IGFBP-1 phosphorylation

The IGF-1R, a transmembrane receptor tyrosine kinase is responsible for mediating IGF-I bioactivity. Binding of IGF-I to the IGF-1R induces receptor autophosphorylation on multiple tyrosine residues on the intracellular IGF-1Rβ subunit. To investigate the effect of the increased IGFBP-1 phosphorylation in response to low oxygen and leucine deprivation on IGF-I bioactivity, we assessed IGF-1Rβ autophosphorylation (Fig. 11A). We utilized IGF-1R over-expressing P6 cells, in which stimulation by IGF-I results in a robust autophosphorylation of the IGF-1Rβ subunit on specific (Tyr1135) residues (Abu Shehab et al., 2013). Fig. 11B in Lane 1 shows that there was minimal (5%) phosphorylation in P6 cells treated with no IGF-I. The presence of IGF-I (100 ng) alone in P6 cells stimulated IGF-1R (100%) (Lane 2). Next, treatment of P6 cells with equimolar concentration IGF-I (100 ng) and total IGFBP-1 (100 ng) from control decidualized HIESC led to a significant reduction (−70%) in IGF-1Rβ autophosphorylation compared to receptor stimulation using IGF-I alone (100%). When P6 cells were treated with IGF-I + IGFBP-1 from cell media of decidualized HIESC incubated under low-oxygen tension additional reduction (−90%) of IGF-1R activation was observed. We attributed these effects due to greater degree of IGFBP-1 phosphorylation in low oxygen tension. Similarly, treatment of P6 cells with IGF-I + IGFBP-1 from cell media of HIESC treated in leucine deprivation caused −95% inhibition of IGF-1R autophosphorylation compared to 100% stimulation with IGF-I alone. Cell media with leucine (Leu 450 μM) also reduced IGF-1R activation (−85%) similar to the control. Levels of total IGF-1Rβ remained unchanged in all conditions. The design of the study utilizing equimolar concentration of IGF-I and IGFBP-1 in each case confirms that these inhibitory effects were not caused by increase in total IGFBP-1 levels or due to a decrease in the amount of receptor protein. Furthermore, the data indicate that increased decidual IGFBP-1 phosphorylation due to cellular stress stimulus exerts inhibitory actions on IGF-1R due to decreased IGF-I bioavailability.

3.8. Status of IGF-1 signaling activity

Furthermore, signals from the IGF-1R and the IR family promote cell growth, survival, adhesion, and motility. Cellular effects of IGF-I are elicited through IGF-I signaling leading to phosphorylation of multiple substrates in downstream intracellular pathway (O'Connor, 2003; Esposito et al., 2001). To determine IGF-I signaling activity in this study we assessed

phosphorylation of IRS-1 at Tyr612 and Akt at Thr308. Fig. 11C and D shows that the phosphorylation of Akt and the phosphorylation of IRS-I was significantly decreased due to possibly increased IGFBP-1 phosphorylation in HIESC cells in response low oxygen or leucine deprivation. However, total IRS-1 and Akt expression levels were similar in control and treated groups.

4. Discussion

Placental insufficiency, the most common cause of FGR and preeclampsia are two important pregnancy complications which are thought to be associated with placental and decidual hypoxia and/or nutrient deprivation. Using cultured HIESC, this study demonstrates for the first time that decidual IGFBP-1 phosphorylation is markedly increased at the three major phosphopeptides (with pSer98/pSer101, pSer119 and pSer169/pSer174) in response to hypoxia or leucine deprivation. Importantly, increased IGFBP-1 phosphorylation led to significantly reduced IGF-I bioactivity. Notably, we also discovered a novel IGFBP-1 phosphorylation site Ser58, highly acidic in nature, which has not been reported in any other biological system. Immunoblotting and immunofluorescence using our custom made extensively validated (Abu Shehab et al., 2014; Abu Shehab et al., 2013) site-specific IGFBP-1 (pSer101, pSer119 and pSer169) antibodies corroborated MRM-MS findings. Together, these data are consistent with the model that decidual IGFBP-1 hyperphosphorylation plays a central role in modulating the IGF-I bioactivity at the maternal and fetal interface representing a critical factor to the development of FGR.

The IGF system comprises of six IGFBPs that can inhibit and/or potentiate IGF activity (Baxter, 2000). At the maternal-fetal interface, IGFBP-1 is important for regulating cellular growth and development by directly binding IGF-I and limiting trophoblast invasion and migration (Irwin and Giudice, 1998). Decidualization is associated with the induction of the IGFBP-1 gene (Tamura et al., 2012) and IGFBP-1 is therefore highly expressed in decidualized endometrial stromal cells *in vivo* and *in vitro* (Martina et al., 1997). The IGFBP-1 promoter contains a cAMP response element for the induction of IGFBP-1 gene expression (Tazuke et al., 1998). The decidualization is dependent upon progesterone signaling and increased cyclic AMP (Westwood et al., 1997), resulting in the secretion of IGFBP-1. Here, we utilized HIESC which are transformed with SV40 large T antigens (Chapdelaine et al., 2006) as a substitute for primary cells. Using morphological (shape index) and functional (characteristic changes in ERα and IGFBP-1 expression and phosphorylation) we confirmed decidualization of HIESC using cAMP + MPA, consistent with previous reports (Westwood et al., 1997).

The mechanisms regulating the secretion and phosphorylation of decidual IGFBP-1 are largely unknown. In this study, HIESC were cultured in low oxygen tension and leucine deprivation to replicate conditions of utero-placental insufficiency. Oxygen tensions in the intervillous space is ~17.9 mm Hg (2.35% O_2) in the first trimester, which increases rapidly to 60 mm Hg (7.9% O_2) once utero-placental circulation is established (Genbacev et al., 1997). We used 1% O_2 to represent low-oxygen/hypoxia whereas room air (20% O_2) for standard cell culture conditions (Simon and Keith, 2008). The rationale for leucine deprivation is that leucine is one of the three branched chain essential amino acids that are

unique in its ability to stimulate protein synthesis (Anthony et al., 2001). Leucine has several times greater impact on protein synthesis than any other amino acid. The 450 μM Leu for HIESC culture is equivalent to normal DMEM/F-12 routinely used *in vitro* (Seferovic et al., 2009; Malkani et al., 2016, 2015).

Previous studies have reported phosphorylated decidual IGFBP-1 at the maternal fetal interface consistent with a role in regulating the IGF-I bioavailability and, as a consequence, placental function (Westwood et al., 1997; Crossey et al., 2002). Phosphorylation of IGFBP-1 (Jones et al., 1993a; Seferovic et al., 2009; Damerill et al., 2016; Jones et al., 1993b; Dolcini et al., 2009) has been previously reported at Ser101 and Ser119, in the mid region and Ser169 at the C-terminal as well as at minor sites Ser95, Ser98 and Ser174 (Damerill et al., 2016). MRM-MS data in this study demonstrate phosphorylation at three major sites (Ser101,119 and 169) of which, two residues are dually phosphorylated. Bioinformatics reveals that IGFBP-1 can be phosphorylated at these sites by multiple protein kinases such as, PKA, PKC and CK2 (Malkani et al., 2016; Ankrapp et al., 1996; Frost and Tseng, 1991). Nonetheless, our previous data showed that Ser101 and Ser169 are within the consensus sequences for CK2 (Malkani et al., 2016) while the kinase responsible for Ser101 phosphorylation is yet to be identified.

Phosphorylation at all three major sites of IGFBP-1 in HIESCs was significantly enhanced in response to low oxygen tension/leucine deprivation. Our MRM-MS data show that the doubly phosphorylated peptide (Ser169/Ser174) elutes first suggesting it to be most negatively charged while the single phosphorylated peptides (Ser98 and Ser101) eluted at the end indicating they were least negatively charged (Table 1). Given that we previously have demonstrated, using BIACORE analysis, that the most negatively charged phosphopeptides contributed to highest binding affinity for IGF-I (Nissum et al., 2009), the current data are intriguing as phosphorylation at most negatively charged Ser169/Ser174 was highly induced in both low oxygen tension and leucine privation. These data suggest the biological relevance of phosphorylation at Ser169/Ser174 potentially to be key in reducing IGF-I bioavailability under cellular stress conditions.

The responsiveness of the three major IGFBP-1 phosphorylation sites individually, to both low oxygen tension/leucine deprivation was confirmed by western blot analysis. The increases in phosphorylation at Ser101/Ser119/pSer169 corroborate the MRM-MS findings. Furthermore, given that the PKA pathway is activated by cAMP, which is required for progesterone dependent decidual cell integrity (Blanks and Brosens, 2012), we targeted the peptide CARGL*pS*CR. This 8 amino acid peptide is followed by the basic amino acid arginine (Arg) allowing Ser58 to be a target for either PKC (pS/T-X-R/K) or PKA (R/K-R/K-X-pS/T) (Malkani et al., 2016). Consistent with this prediction, MRM-MS validated pSer58 as a novel IGFBP-1 phosphorylation site. Although pSer58 was not affected by low oxygen tension or leucine deprivation, it is possible that Ser58 has a yet unrecognized function. Structurally, 12 cysteines clustered at the conserved N-terminal third of IGFBP-1 are essential for IGF-I binding (Forbes et al., 2012). We speculate that phosphorylation at Ser58 may consequently lead to changes in IGF-I binding due to unique attributes of the N-terminal domain. Furthermore, the peptides between amino acids 26–107 are rich in Ser/Thr residues resulting in a high potential for more phosphorylation events that may contribute to

enhance or inhibit IGF-I binding. The biological significance of phosphorylation of Ser58 remains undefined but is likely to affect binding to IGF-I.

Additionally, vimentin has been recognized as a marker for epithelial-mesenchymal cells (Liu et al., 2015) and decidual cells expresses vimentin (Trenkic et al., 2008). Decidual localization of IGFBP-1 has been reported previously (Fowler et al., 2000; Mottet et al., 2005; Brar et al., 1997). The dual immunostaining with anti-vimentin antibody showed decidual stromal cells with overlapping IGFBP-1 phosphorylation (Ser101/Ser119 and Ser169) in the cytoplasm. Further, we provide additional novel information showing increases in all three decidual cytoplasmic IGFBP-1 phosphoisoforms in response to low oxygen tension/leucine deprivation. The three known residues play a major functional role in IGF-I binding (Nissum et al., 2009), suggests a strongly controlled action of IGFBP-1 phosphorylation in reducing IGF-I bioavailability in decidual cells in response to hypoxia or/and decreased nutrient availability consistent with placental insufficiency.

The physiological relevance of IGFBP-1 phosphorylation in our study is additionally supported by the demonstration that increased phosphorylation in hypoxia/leucine deprivation reduces IGF-1R autophosphorylation and down regulates IGF-I signaling. An up-regulation of phosphorylation of IRS-1 has been reported previously during HESC decidualization (Ganeff et al., 2009). Here, using functional readouts, we showed that the activity of the proximal IGF-I signaling pathway was inhibited mainly due to hyperphosphorylation of IGFBP-1.

Although leucine deprivation or hypoxia show similar effects, high sensitivity of MRM-MS demonstrated relatively greater increase in IGFBP-1 phosphorylation in response to low oxygen tension. Viewed together, these findings suggest that the subtle differences between the two treatments may be linked to both common and/or unique sets of regulatory mechanisms. Further investigation is necessary for distinguishing intracellular oxygen and nutrient sensing signaling pathways involved in modulating decidual IGFBP-1 phosphorylation under two different cellular stress conditions.

In summary, the present findings provide compelling new evidence for an important role of low oxygen tension and/or amino acid levels in modulating site specific decidual IGFBP-1 phosphorylation. It is plausible that *in-vitro* studies with HIESC do not reflect the real complexity of placental insufficiency, nonetheless these findings suggest a central role of IGFBP-1 hyperphosphorylation in modulating the IGF-I action at the maternal-fetal interface representing a critical factor to the development of FGR. It is likely that a decreased availability of oxygen and amino acids constitute two key changes ‘sensed’ by the decidua in FGR. Identifying the respective molecular pathways is an essential next step in advancing our understanding of the nutrient and oxygen sensing signaling mechanisms that link the two stress stimuli to decidual IGFBP-1 hyperphosphorylation that may lead to FGR with long-term adverse outcomes in growth restricted infants.

Supplementary Material

Refer to Web version on PubMed Central for supplementary material.

Acknowledgments

This work was supported in part by the Natural Science and Engineering Council of Canada Discovery grant (NSERC, RGPIN-2016-04752; RGPIN-2015-05000) and Lawson Health Research Institute (HRF0512) to MBG. We thank Dr. Michel A. Fortier, Faculté de Médecine, Université Laval, Sainte-Foy, Québec, Canada for his kind gift of human endometrial stromal cells. We also thank Dr. Rob Baxter for his kind gift of IGFBP-1 polyclonal antibody and Biotron Integrated Microscopy, University of Western Ontario for providing facility to conduct dual immunofluorescent analyses.

References

Abu Shehab M, Inoue S, Han VK, Gupta MB. Site specific phosphorylation of insulin-like growth factor binding protein-1 (IGFBP-1) for evaluating clinical relevancy in fetal growth restriction. J Proteome Res. 2009; 8:5325–5335. [PubMed: 19731965]

Abu Shehab M, Khosravi J, Han VK, Shilton BH, Gupta MB. Site-specific IGFBP-1 hyper-phosphorylation in fetal growth restriction: clinical and functional relevance. J Proteome Res. 2010; 9:1873–1881. [PubMed: 20143870]

Abu Shehab M, Iosef C, Wildgruber R, Sardana G, Gupta MB. Phosphorylation of IGFBP-1 at discrete sites elicits variable effects on IGF-1 receptor autophosphorylation. Endocrinology. 2013; 154:1130–1143. [PubMed: 23354097]

Abu Shehab M, Damerill I, Shen T, Rosario FJ, Nijland M, Nathanielsz PW, Kamat A, Jansson T, Gupta MB. Liver mTOR controls IGF-I bioavailability by regulation of protein kinase CK2 and IGFBP-1 phosphorylation in fetal growth restriction. Endocrinology. 2014; 155:1327–1339. [PubMed: 24437487]

Ankrapp DP, Jones JI, Clemmons DR. Characterization of insulin-like growth factor binding protein-1 kinases from human hepatoma cells. J Cell Biochem. 1996; 60:387–399. [PubMed: 8867814]

Anthony JC, Anthony TG, Kimball SR, Jefferson LS. Signaling pathways involved in translational control of protein synthesis in skeletal muscle by leucine. J Nutr. 2001; 131:856s–860s. [PubMed: 11238774]

Averous J, Maurin AC, Bruhat A, Jousse C, Arliguie C, Fafournoux P. Induction of IGFBP-1 expression by amino acid deprivation of HepG2 human hepatoma cells involves both a transcriptional activation and an mRNA stabilization due to its 3′UTR. FEBS Lett. 2005; 579:2609–2614. [PubMed: 15862298]

Baker J, Liu JP, Robertson EJ, Efstratiadis A. Role of insulin-like growth factors in embryonic and postnatal growth. Cell. 1993; 75:73–82. [PubMed: 8402902]

Baxter RC. Insulin-like growth factor (IGF)-binding proteins: interactions with IGFs and intrinsic bioactivities. Am J Physiol Endocrinol Metab. 2000; 278:E967–E976. [PubMed: 10826997]

Blanks AM, Brosens JJ. Progesterone action in the myometrium and decidua in preterm birth. Facts, Views Vis ObGyn. 2012; 4:33–43. [PubMed: 24753902]

Brar AK, Frank GR, Kessler CA, Cedars MI, Handwerger S. Progesterone-dependent decidualization of the human endometrium is mediated by cAMP. Endocrine. 1997; 6:301–307. [PubMed: 9368687]

Chapdelaine P, Kang J, Boucher-Kovalik S, Caron N, Tremblay JP, Fortier MA. Decidualization and maintenance of a functional prostaglandin system in human endometrial cell lines following transformation with SV40 large T antigen. Mol Hum Reprod. 2006; 12:309–319. [PubMed: 16556676]

Chellakooty M, Vangsgaard K, Larsen T, Scheike T, Falck-Larsen J, Legarth J, Andersson AM, Main KM, Skakkebaek NE, Juul A. A longitudinal study of intrauterine growth and the placental growth hormone (GH)-insulin-like growth factor I axis in maternal circulation: association between placental GH and fetal growth. J Clin Endocrinol Metab. 2004; 89:384–391. [PubMed: 14715876]

Crossey PA, Pillai CC, Miell JP. Altered placental development and intra-uterine growth restriction in IGF binding protein-1 transgenic mice. J Clin Invest. 2002; 110:411–418. [PubMed: 12163461]

Damerill I, Biggar KK, Abu Shehab M, Li SS, Jansson T, Gupta MB. Hypoxia increases IGFBP-1 phosphorylation mediated by mTOR inhibition. Mol Endocrinol (Baltim, Md). 2016; 30:201–216.

Dolcini L, Sala A, Campagnoli M, Labo S, Valli M, Visai L, Minchiotti L, Monaco HL, Galliano M. Identification of the amniotic fluid insulin-like growth factor binding protein-1 phosphorylation sites and propensity to proteolysis of the isoforms. FEBS J. 2009; 276:6033–6046. [PubMed: 19765076]

Esposito DL, Li Y, Cama A, Quon MJ. Tyr(612) and Tyr(632) in human insulin receptor substrate-1 are important for full activation of insulin-stimulated phosphatidylinositol 3-kinase activity and translocation of GLUT4 in adipose cells. Endocrinology. 2001; 142:2833–2840. [PubMed: 11416002]

Firth SM, Baxter RC. Cellular actions of the insulin-like growth factor binding proteins. Endocr Rev. 2002; 23:824–854. [PubMed: 12466191]

Forbes BE, McCarthy P, Norton RS. Insulin-like growth factor binding proteins: a structural perspective. Front Endocrinol. 2012; 3:38.

Fowler DJ, Nicolaides KH, Miell JP. Insulin-like growth factor binding protein-1 (IGFBP-1): a multifunctional role in the human female reproductive tract. Hum Reprod Update. 2000; 6:495–504. [PubMed: 11045880]

Frost RA, Tseng L. Insulin-like growth factor-binding protein-1 is phosphorylated by cultured human endometrial stromal cells and multiple protein kinases in vitro. J Biol Chem. 1991; 266:18082–18088. [PubMed: 1655736]

Ganeff C, Chatel G, Munaut C, Frankenne F, Foidart JM, Winkler R. The IGF system in in-vitro human decidualization. Mol Hum Reprod. 2009; 15:27–38. [PubMed: 19038974]

Genbacev O, Zhou Y, Ludlow JW, Fisher SJ. Regulation of human placental development by oxygen tension. Science. 1997; 277:1669–1672. [PubMed: 9287221]

Gibson JM, Aplin JD, White A, Westwood M. Regulation of IGF bioavailability in pregnancy. Mol Hum Reprod. 2001; 7:79–87. [PubMed: 11134364]

Gluckman PD, Pinal CS. Regulation of fetal growth by the somatotrophic axis. J Nutr. 2003; 133:1741s–1746s. [PubMed: 12730493]

Gluckman PD, Hanson MA, Cooper C, Thornburg KL. Effect of in utero and early-life conditions on adult health and disease. N Engl J Med. 2008; 359:61–73. [PubMed: 18596274]

Hutter D, Kingdom J, Jaeggi E. Causes and mechanisms of intrauterine hypoxia and its impact on the fetal cardiovascular system: a review. Int J Pediatr. 2010; 2010:401323. [PubMed: 20981293]

Irwin JC, Giudice LC. Insulin-like growth factor binding protein-1 binds to placental cytotrophoblast alpha5beta1 integrin and inhibits cytotrophoblast invasion into decidualized endometrial stromal cultures. Growth Horm IGF Res. 1998; 8:21–31.

Jones JI, Busby WH Jr, Wright G, Clemmons DR. Human IGFBP-1 is phosphorylated on 3 serine residues: effects of site-directed mutagenesis of the major phosphoserine. Growth Regul. 1993; 3:37–40. [PubMed: 7683525]

Jones JI, Busby WH Jr, Wright G, Smith CE, Kimack NM, Clemmons DR. Identification of the sites of phosphorylation in insulin-like growth factor binding protein-1. Regulation of its affinity by phosphorylation of serine 101. J Biol Chem. 1993; 268:1125–1131. [PubMed: 7678248]

Kajihara T, Tanaka K, Oguro T, Tochigi H, Prechapanich J, Uchino S, Itakura A, Sucurovic S, Murakami K, Brosens JJ, Ishihara O. Androgens modulate the morphological characteristics of human endometrial stromal cells decidualized in vitro. Reproductive Sci (Thousand Oaks, Calif). 2014; 21:372–380.

Kajimura S, Aida K, Duan C. Insulin-like growth factor-binding protein-1 (IGFBP-1) mediates hypoxia-induced embryonic growth and developmental retardation. Proc Natl Acad Sci U S A. 2005; 102:1240–1245. [PubMed: 15644436]

Liu CY, Lin HH, Tang MJ, Wang YK. Vimentin contributes to epithelial-mesenchymal transition cancer cell mechanics by mediating cytoskeletal organization and focal adhesion maturation. Oncotarget. 2015; 6:15966–15983. [PubMed: 25965826]

Malkani N, Biggar K, Abu Shehab M, Li S, Jansson T, Gupta MB. Increased IGFBP-1 phosphorylation in response to leucine deprivation is mediated by CK2 and PKC. Mol Cell Endocrinol. 2016; 425:48–60. [PubMed: 26733150]

Malkani N, Jansson T, Gupta MB. IGFBP-1 hyperphosphorylation in response to leucine deprivation is mediated by the AAR pathway. Mol Cell Endocrinol. 2015; 412:182–195. [PubMed: 25957086]

Martina NA, Kim E, Chitkara U, Wathen NC, Chard T, Giudice LC. Gestational age-dependent expression of insulin-like growth factor-binding protein-1 (IGFBP-1) phosphoisoforms in human extraembryonic cavities, maternal serum, and decidua suggests decidua as the primary source of IGFBP-1 in these fluids during early pregnancy. J Clin Endocrinol metabolism. 1997; 82:1894–1898.

Mottet D, Ruys SP, Demazy C, Raes M, Michiels C. Role for casein kinase 2 in the regulation of HIF-1 activity. Int J Cancer. 2005; 117:764–774. [PubMed: 15957168]

Nissum M, Abu Shehab M, Sukop U, Khosravi JM, Wildgruber R, Eckerskorn C, Han VK, Gupta MB. Functional and complementary phosphorylation state attributes of human insulin-like growth factor-binding protein-1 (IGFBP-1) isoforms resolved by free flow electrophoresis. Mol Cell Proteomics: MCP. 2009; 8:1424–1435. [PubMed: 19193607]

O'Connor R. Regulation of IGF-1 receptor signaling in tumor cells. Horm Metab Res = Horm- und Stoffwechselforschung = Horm Metab. 2003; 35:771–777.

Popovici RM, Lu M, Bhatia S, Faessen GH, Giaccia AJ, Giudice LC. Hypoxia regulates insulin-like growth factor-binding protein 1 in human fetal hepatocytes in primary culture: suggestive molecular mechanisms for in utero fetal growth restriction caused by uteroplacental insufficiency. J Clin Endocrinol Metab. 2001; 86:2653–2659. [PubMed: 11397868]

Seferovic MD, Gupta MB. Increased umbilical cord PAI-1 levels in placental insufficiency are associated with fetal hypoxia and angiogenesis. Dis markers. 2016; 2016:7124186. [PubMed: 26903689]

Seferovic MD, Ali R, Kamei H, Liu S, Khosravi JM, Nazarian S, Han VK, Duan C, Gupta MB. Hypoxia and leucine deprivation induce human insulin-like growth factor binding protein-1 hyperphosphorylation and increase its biological activity. Endocrinology. 2009; 150:220–231. [PubMed: 18772238]

Seferovic MD, Chen S, Pinto DM, Gupta MB. Altered liver secretion of vascular regulatory proteins in hypoxic pregnancies stimulate angiogenesis in vitro. J Proteome Res. 2011; 10:1495–1504. [PubMed: 21319863]

Simon MC, Keith B. The role of oxygen availability in embryonic development and stem cell function. Nat Rev Mol cell Biol. 2008; 9:285–296. [PubMed: 18285802]

Tamura I, Asada H, Maekawa R, Tanabe M, Lee L, Taketani T, Yamagata Y, Tamura H, Sugino N. Induction of IGFBP-1 expression by cAMP is associated with histone acetylation status of the promoter region in human endometrial stromal cells. Endocrinology. 2012; 153:5612–5621. [PubMed: 23011923]

Tazuke SI, Mazure NM, Sugawara J, Carland G, Faessen GH, Suen LF, Irwin JC, Powell DR, Giaccia AJ, Giudice LC. Hypoxia stimulates insulin-like growth factor binding protein 1 (IGFBP-1) gene expression in HepG2 cells: a possible model for IGFBP-1 expression in fetal hypoxia. Proc Natl Acad Sci U S A. 1998; 95:10188–10193. [PubMed: 9707622]

Trenkic M, Basic M, Milentijevic M, Petrovic A, Zivkovic V, Lazarevic V. Immunohistohemical evidences of pregnancy in uterine curettage tissue by the use of a double immunocytochemical staining technique using cytokeratin 7 and vimentin antibodies. Vojnosanit Pregl. 2008; 65:810–813. [PubMed: 19069710]

Watson CS, Bialek P, Anzo M, Khosravi J, Yee SP, Han VK. Elevated circulating insulin-like growth factor binding protein-1 is sufficient to cause fetal growth restriction. Endocrinology. 2006; 147:1175–1186. [PubMed: 16293667]

Westwood M, Gibson JM, White A. Purification and characterization of the insulin-like growth factor-binding protein-1 phosphoform found in normal plasma. Endocrinology. 1997; 138:1130–1136. [PubMed: 9048619]

Appendix A. Supplementary data

Supplementary data related to this article can be found at http://dx.doi.org/10.1016/j.mce.2017.04.005.

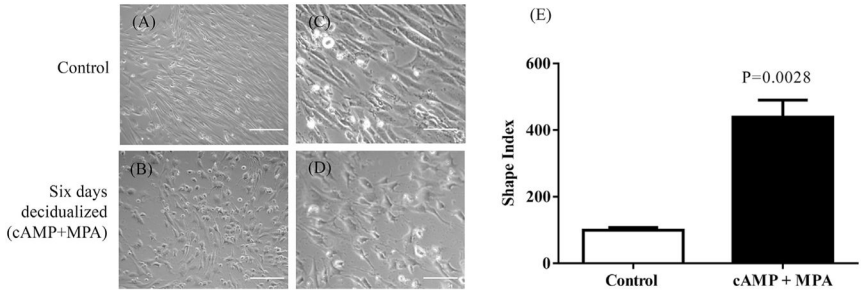

Fig. 1. Morphological characteristics of HIESC during *in vitro* decidualization

Changes in morphology following six days decidualization of HIESCs using combined cAMP + MPA treatments. Non decidualized HIESCs remained elongated spindle shaped throughout the culture period (A, 10x and C, 20x). Cells treated with cAMP + MPA acquired an ovoid shaped morphology indicative of decidualization (B, 10x, D, 20X). The shape index determined for HIESCs culture system using image analysis software and calculated using the formula: 4 P -area/perimeter^2. A circle wound has a shape index of 1 and a straight line has an index of 0. The shape indexes were calculated from ~50 cells from 3 sets of samples to quantify morphologic changes. (E) Shows undecidualized HIESCs have a mean ± SEM shape index of 100% (control), while the decidualized cells have a mean ± SEM shape index of 439.5%. The mean ± SEM shape index of decidualized samples (n = 3) in triplicates were compared to undecidualized cells by Student T test and considered significant at $P < 0.05$.

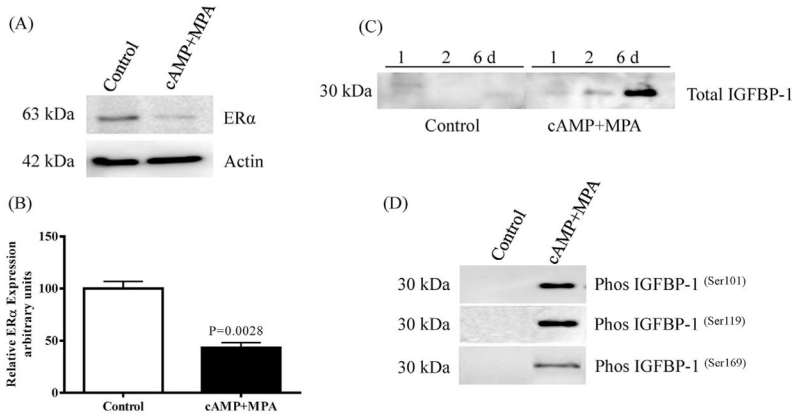

Fig. 2. Evaluation of decidualized HIESC

Expression of ERα in cellular extract of HIESC detected by immunoblotting showed mean ± SEM significant ($P < 0.05$) down regulation upon decidualization (A and B). Total IGFBP-1 secretion in cell media was detectable at 24 h treatment of cells with cAMP + MPA and reached a maximum peak by six days (C). Western blot analysis using equal aliquots of cell media of undecidualized HIESCs (untreated) control (n = 3) and cAMP + MPA -treated cells (n = 3) for six days showed decidualization of HIESCs concomitantly increased IGFBP-1 phosphorylation at the indicated 3 Ser residues.

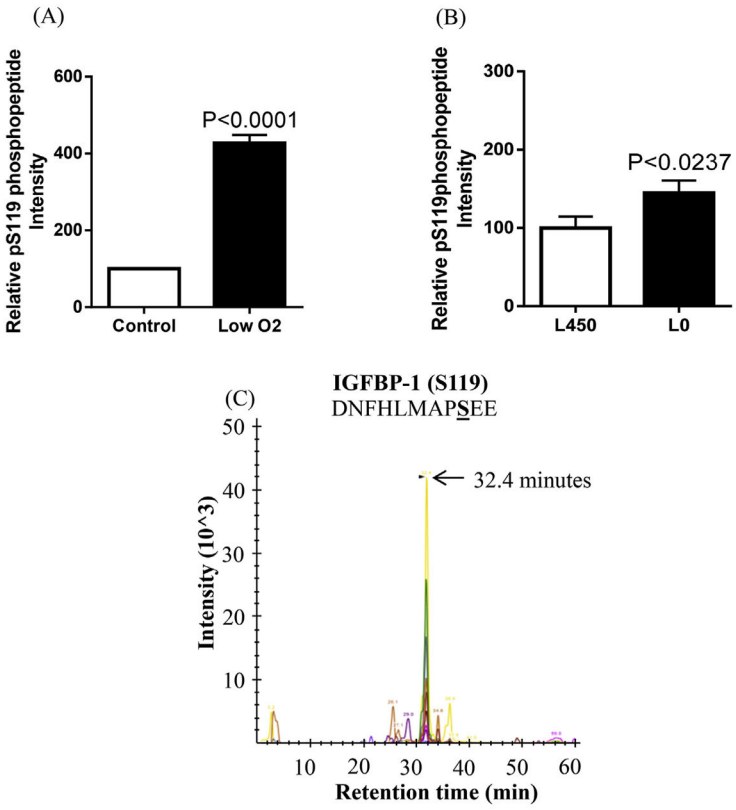

Fig. 3. MRM/MS analysis of IGFBP-1 phosphorylation at Ser119

Phosphorylation of IGFBP-1 at Ser119 was enhanced in response to low oxygen tension (A) compared to normoxia and/or leucine deprivation (Leu 0 μM) vs control (Leu 450 μM) (B) in decidualized HIESC cell media. The data is a representative of pooled triplicates from two separate biological treatments. Depiction of the extracted ion chromatographs showing the transitions used to validate the phosphorylation at pS119 (C) (AB SCIEX QTRAP 4000 linear ion trap mass spectrometer).

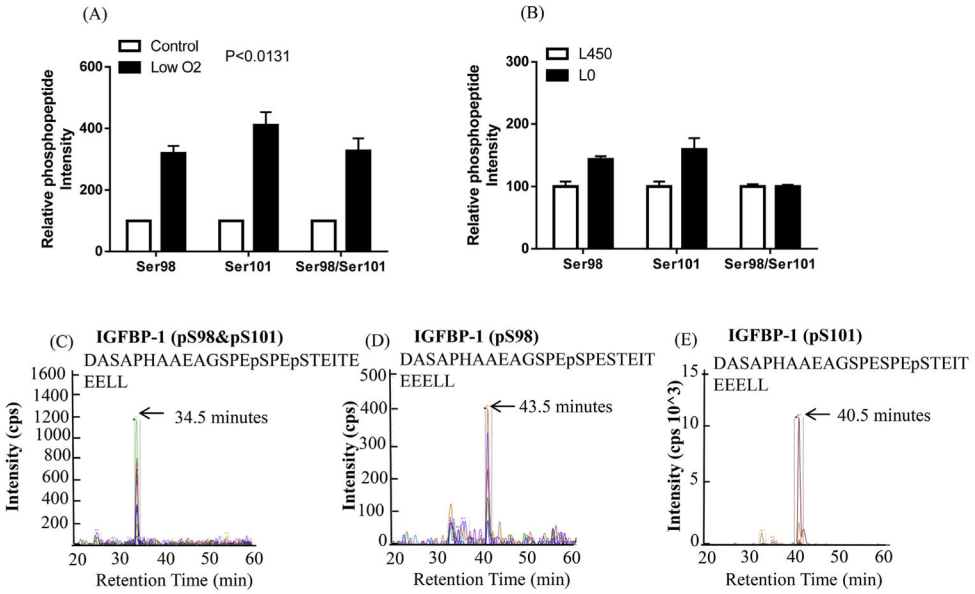

Fig. 4. MRM/MS analysis of IGFBP-1 phosphorylation at Ser98/Ser101

Phosphorylation of IGFBP-1 at Ser98 and/or Ser101 was enhanced in response to low oxygen tension (A) compared to its respective control normoxia and/or leucine deprivation (Leu 0 μM) vs control (Leu 450 μM) (B) in decidualized HIESC cell media. The data is representative of pooled triplicates from two separate biological treatments. In some groups the SEM was small and did not extend beyond the bar. Depiction of the extracted ion chromatographs showing the transitions used to validate the phosphorylation at Ser98 and/or Ser101 (C–E) in doubly phosphorylated peptides (AB SCIEX QTRAP 4000 linear ion trap mass spectrometer).

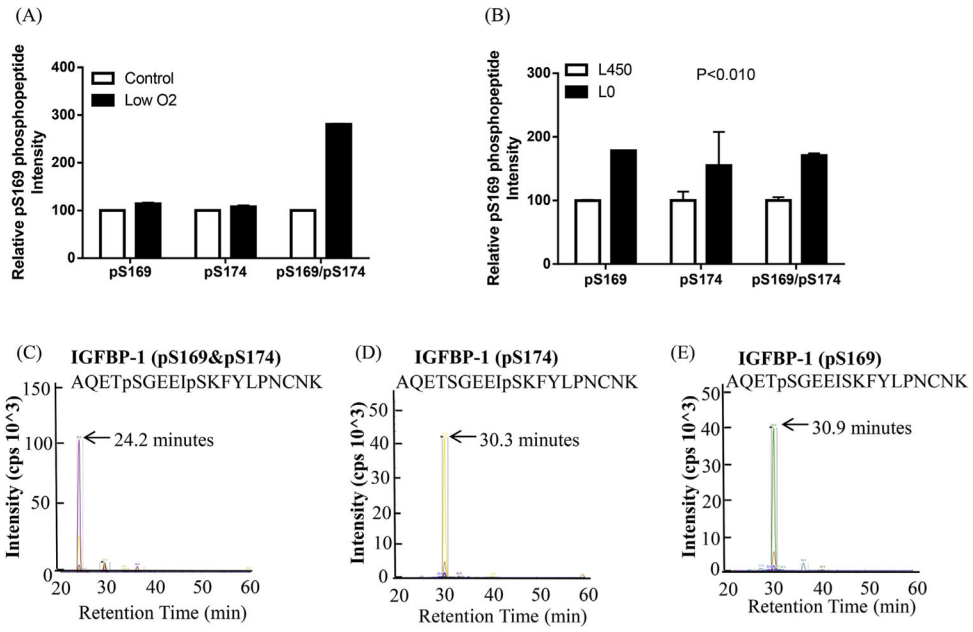

Fig. 5. MRM/MS analysis of IGFBP-1 phosphorylation at pSer169/pSer174

Phosphorylation of IGFBP-1 at Ser169 and/or Ser174 was enhanced in response to low oxygen tension compared to its respective control normoxia (A) and/or leucine deprivation (L0) vs control (Leu 450 μM) (B) in decidualized HIESC cell media. The data is a representative of pooled triplicates from two separate biological treatments. In some groups the SEM was small and did not extend beyond the bar. Depiction of the extracted ion chromatographs showing the transitions used to validate the phosphorylation at pS169 and/or PS174 (C–E) in doubly phosphorylated peptides (AB SCIEX QTRAP 4000 linear ion trap mass spectrometer).

APWQCAPCSA EKLALCPPVS ASCSEVTRSA GCGCCPMCALP
LGAACGVATA **R**CA**R**GL**S**C**R**AL PGEQQPLHAL TRGQGACVQE

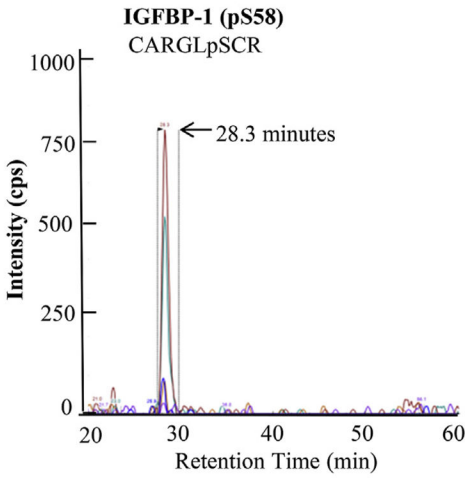

Fig. 6. MRM/MS identification of pSer58 as novel phosphorylation site

Depiction of the extracted ion chromatographs showing the transitions used to validate the phosphorylation of IGFBP-1 at newly identified pSer58 in decidualized HIESCs which was not effected in response to hypoxia or leucine deprivation. (SCIEX QTRAP 4000 linear ion trap mass spectrometer).

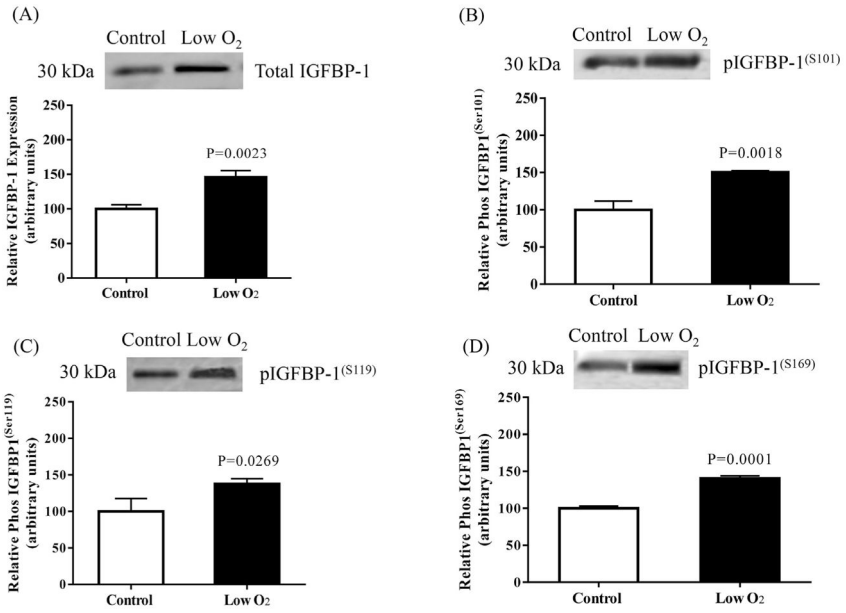

Fig. 7. The effect of low oxygen tension on IGFBP-1 secretion and phosphorylation

Representative Western blot of total and phosphorylated IGFBP-1 secreted by decidualized HIESCs from control (normoxia) (n = 3) and hypoxia treated cells (n = 3). Equal volume of cell media from control and hypoxia treated cells was subjected to immunoprecipitation using anti human IGFBP-1 monoclonal antibody (mAb 6303) and tested for total (A) and phosphorylated IGFBP-1$^{(S101)}$ (B) IGFBP-1$^{(S119)}$ (C) and IGFBP-1$^{(S169)}$ (D). Low oxygen treatment significantly increased IGFBP-1 secretion and phosphorylation at three serine sites in decidualized HIESCs compared to normoxia. Values are given as means ± SEM. $P < 0.05$ vs control is significant as per unpaired Student *t*-test.

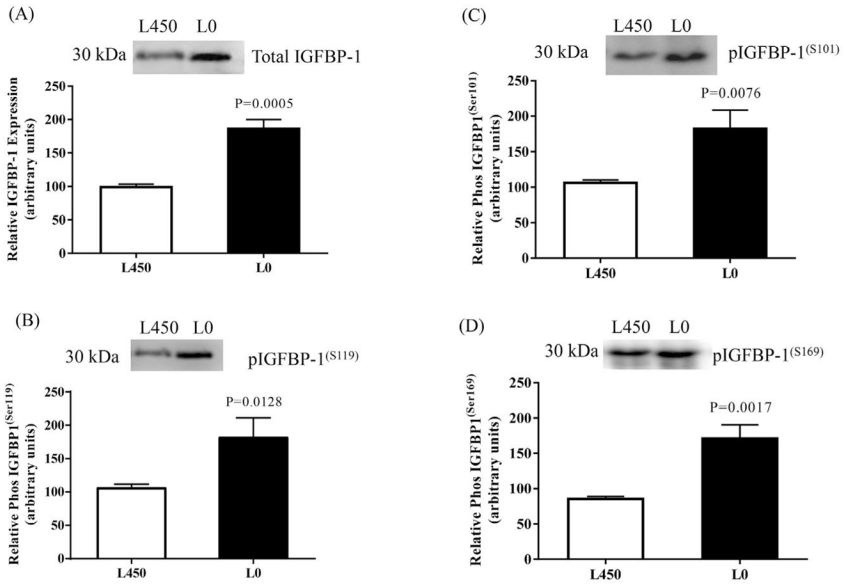

Fig. 8. The effect of leucine deprivation on IGFBP-1 secretion and phosphorylation

Representative Western blot of total and phosphorylated IGFBP-1 secreted by decidualized HIESCs from control (L 450) (n = 3) and leucine deprived cells (24 h) (n = 3). Equal volume of cell media from leucine deprived (L0) or with leucine (L450) was immunoprecipitated using anti human IGFBP-1 monoclonal antibody (mAb 6303) and tested on immunoblot for total (A) and phosphorylated IGFBP-1$^{(S101)}$ (B) IGFBP-1$^{(S119)}$ (C) and IGFBP-1$^{(S169)}$ (D). Leucine deprivation significantly increased IGFBP-1 secretion and phosphorylation at three serine sites in decidualized HIESCs. Values are given as means ± SEM. $P < 0.05$ vs control is significant as per unpaired Student *t*-test.

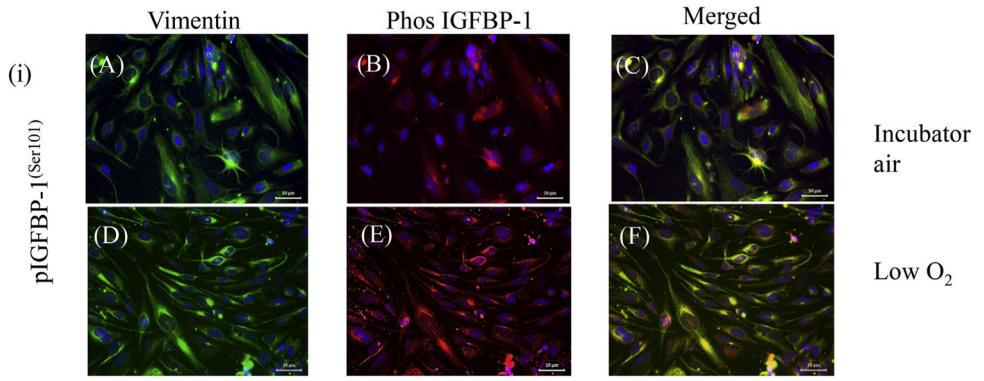

Fig. 9. Dual-immunofluorescence analyses for IGFBP-1 phosphoisoforms in response to low oxygen tension

Dual-immunofluorescence staining depicted the vast majority of decidualized HIESCs to be positive for vimentin (green) in the cytoplasm also localized phos IGFBP-1 (red). HIESCs co-express phosphorylated IGFBP-1$^{(S101)}$ and vimentin (A–F). A higher expression of phosphorylated IGFBP-1 at Ser101 is depicted in response to low oxygen tension (E) compared to incubator air (control) (B). The changes in expression of IGFBP-1 were not attributed to the level of decidualization of cells, which was relatively equal in both conditions as shown by vimentin staining (A and D). Merged superimposed images (co-localization of red and green yields yellow) mainly in the cytoplasm are shown in the last panel (C and F). Nucleus is stained with DAPI (Blue). Scale Bar = 50 μm. (For interpretation of the references to colour in this figure legend, the reader is referred to the web version of this article.)

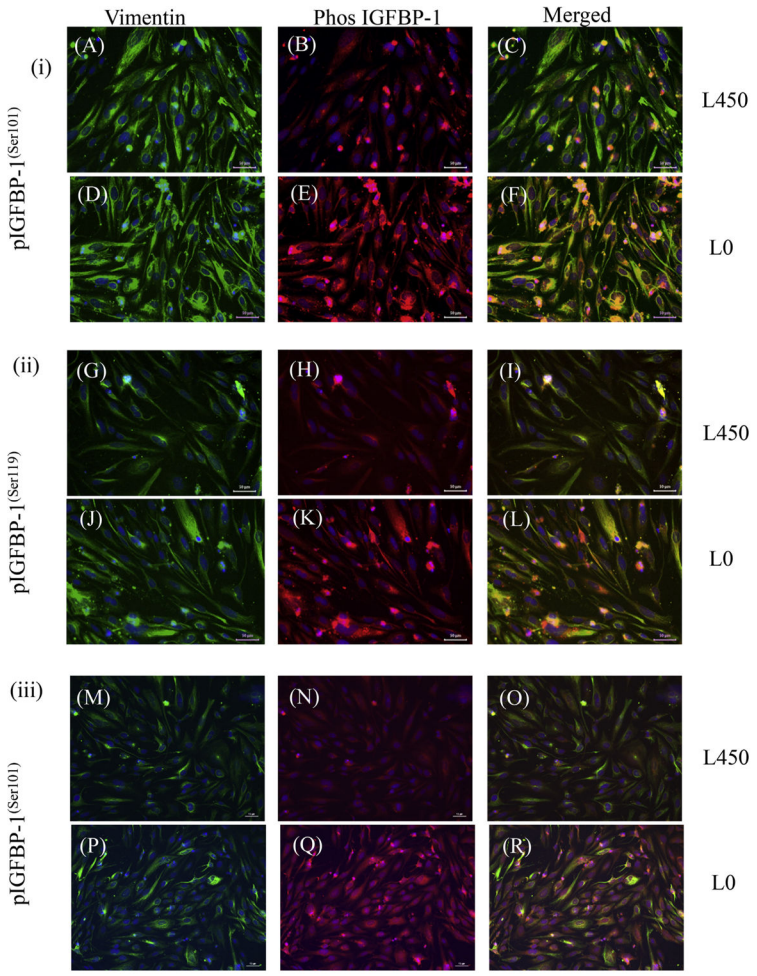

Fig. 10. Dual-immunofluorescence analyses of IGFBP-1 phosphoisoforms in response to leucine deprivation

Dual immunofluorescence staining depicted the vast majority of decidualized HIESCs to be positive for vimentin (green) also localized IGFBP-1 (red). HIESCs express phosphorylated (i) IGFBP-1$^{(S101)}$ and vimentin (A–F); (ii) IGFBP-1$^{(S119)}$ and vimentin (G–L); (iii) IGFBP-1$^{(S169)}$ and vimentin (M–R). A higher expression of phosphorylated IGFBP-1 at Ser101, 119 and 169 is depicted in decidualized cells in response to leucine deprivation (E, K and Q) compared to decidualized cells cultured in media with leucine (B, H and N). The expression changes in IGFBP-1 were not attributed to the level of decidualization of cells, which was relatively equal in both conditions as shown by vimentin staining (A, D, G, J, M and P). Merged superimposed images (co-localization of red and green yields yellow) are shown in the last panel (C, F, I, L, O and R). Nucleus is stained with DAPI (Blue). Scale Bar = 50 μm. (For interpretation of the references to colour in this figure legend, the reader is referred to the web version of this article.)

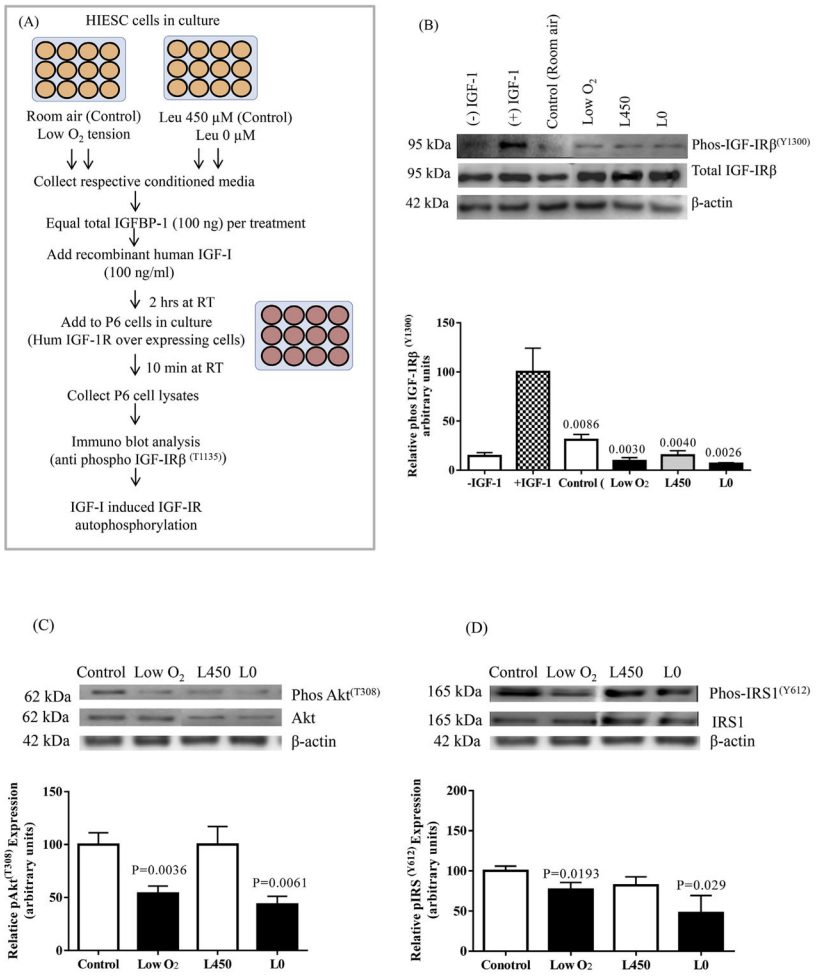

Fig. 11.

The effect of IGFBP-1 hyperphosphorylation on the inhibition of IGF-1 receptor autophosphorylation and IGF-1R downstream signaling. (A) A schematic flow chart summarizing the IGF-1R autophosphorylation assay using P6 cells overexpressing IGF-1R and HIESC cell media from Low O_2 and leucine deprivation experiments.

(B) Representative western blots of phospho IGF-Rβ$^{(Tyr\ 1135)}$ in P6 cell lysate after treatment with control (room air), low oxygen tension and with (L450) and without leucine (L0) treated decidual IGFBP-1. Phosphorylated IGFBP-1 isolated from HIESC treated with low oxygen treatment compared to control (HIESC in room air) significantly inhibited IGF-R activation in P6 cells. Low oxygen tension and leucine deprivation (L0) both contributed to dramatic inhibition of IGF-R activation. After normalization to β-actin, the mean ± SEM band intensity of treated samples was significantly different where indicated ($P < 0.05$) compared to the control samples as per ANOVA.

(C) Representative Western blots for pAkt$^{(Thr308)}$ and pIRS-1$^{(Tyr\ 612)}$ (D) in cell lysate of control (room air), ow oxygen tension and with (L 450)and without leucine (L0). In low oxygen treated and leucine deprived cells phosphorylation of Akt at Thr-308 and phosphorylation of IRS-1 at Tyr-612 was significantly decreased compared to controls while the expression of total Akt and total IRS-1 was similar in both the control and treated cells.

After normalization to β-actin, the mean ± SEM band intensity of treated samples was significantly different where indicated ($P < 0.05$) compared to the control samples as per unpaired Student' T test.

Table 1

Summary of the detected phosphorylation sites within single or double phospho-peptidesrelative to their corresponding retention time as detected by MRM/MS.

Site	Peptide	Retention time
pSer169/pSer174	A QETpSGEEIpSK	25 min
pSer58	RCARGLpSCRAL	28 min
pSer169	A QETpSGEEISK	30 min
pSer174	A QETSGEEIpSK	32 min
pSer119	DNFHLMApSEE	32.5 min
pSer98/pSer101	DASAPHAAEAGSPEpSPEpSTEITEEELL	35 min
pSer98	DASAPHAAEAGSPEpSPESTEITEEELL	40 min
pSer101	DASAPHAAEAGSPESPEpSTEITEEELL	42 min